[JGR Atmospheres]

Supporting Information for

Potential Effect of Halogens on Atmospheric Oxidation and Air Quality in China

Qinyi Li[1], Alba Badia[1], Tao Wang[2], Golam Sarwar[3], Xiao Fu[2], Li Zhang[4,5], Qiang Zhang[6], Jimmy Fung[7], Carlos A. Cuevas[1], Shanshan Wang[8], Bin Zhou[8], and Alfonso Saiz-Lopez[1,8]*

[1] Department of Atmospheric Chemistry and Climate, Institute of Physical Chemistry Rocasolano, CSIC, Madrid 28006, Spain

[2] Department of Civil and Environmental Engineering, The Hong Kong Polytechnic University, Hong Kong, China

[3] National Exposure Research Laboratory, Environmental Protection Agency, Research Triangle Park, NC 27711, United States

[4] Atmospheric and Oceanic Sciences, Princeton University, Princeton, New Jersey 08540, United States

[5] Geophysical Fluid Dynamics Laboratory, National Oceanic and Atmospheric Administration, Princeton, New Jersey, 08544, United States

[6] Department of Earth System Science, Tsinghua University, Beijing 100084, China

[7] Division of Environment and Sustainability, Hong Kong University of Science and Technology, Hong Kong, China

[8] Department of Environmental Science and Engineering, Fudan University, Shanghai 200433, China

* Corresponding author: Alfonso Saiz-Lopez (a.saiz@csic.es)

Contents of this file

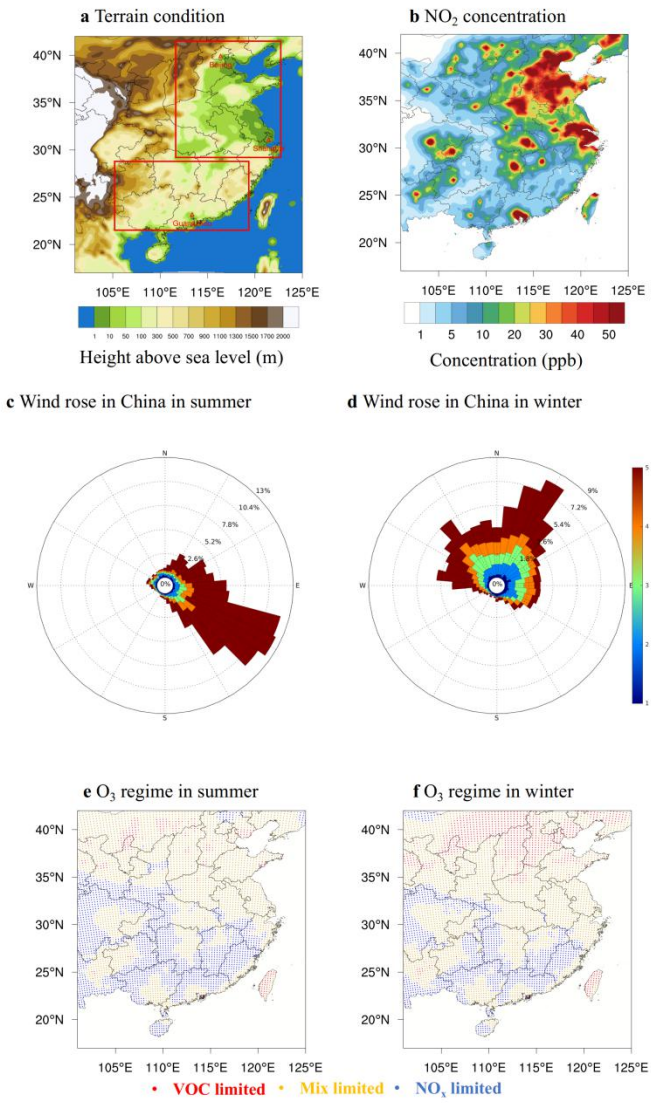

Figure S1 Terrain, chemical, and meteorological conditions within the domain of WRF-Chem simulation. **a** Colour shade represents the height above sea level (m). Red triangles and the associated texts represent the major cities of Beijing, Shanghai, and Guangzhou. The red frame in the north represents the northern part of China, and the red frame in the south is the southern part of China. **b** Annual average of daily-maximum NO_2 at surface in the HAL case. Higher NO_x grids represent the polluted areas (urban and industrial areas) and low NO_x grids are the rural and suburban areas. **c** Wind rose in East China in winter. East China is dominated by northern winds that export the air mass out of the land into the ocean. **d** Wind rose in East China in summer. South to east is the prevailing wind direction which imports the air mass from the ocean into the land. **e**, **f** Distributions of VOC, mixed, and NOx-limited regions in China in summer and winter in the HAL scenario.

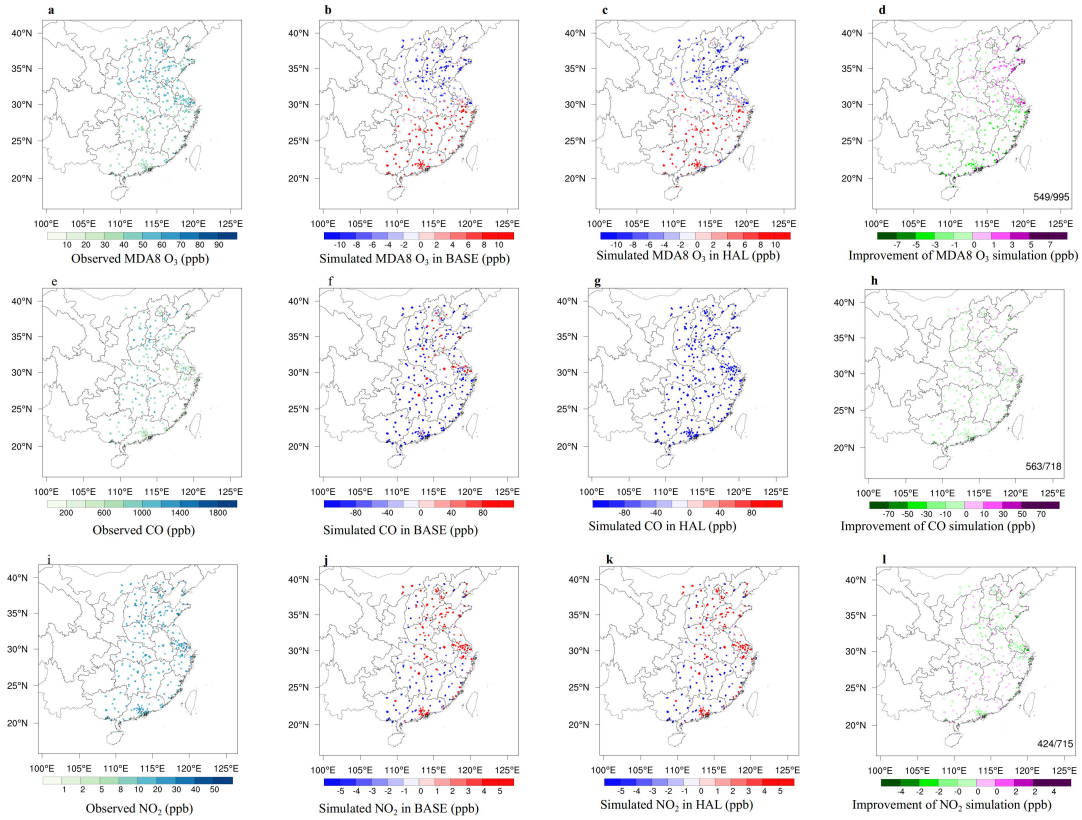

Figure S2 Comparison of the surface O_3, CO, and NO_2 simulations in BASE and HAL cases with the observation in China. All units are in ppb. **a** The averages of the observed maximum daily 8-h average (MDA8) O_3 concentrations. The sites with less than 50% available observations in 2018 are excluded. **b** The differences of MDA8 O_3 between BASE and observation. O_3 in the north is underestimated in the BASE model, possibly due to the lack of some biomass burning emission and domestic cooking sources not captured in the emission inventory. Please note that a fire emission inventory (FINN) is already used in this study. **c** The difference of MDA8 O_3 between HAL and observations. **d** The MDA8 O_3 simulation in HAL compared with that in BASE. Green colour represents better prediction in HAL and purple colour represents worse prediction in HAL; the number ratio at the corner is the number of sites (549) with improved prediction v.s. the number of total sites (995). The HAL scenario improves O_3 simulation in many sites (over 50%) but worsen O_3 predictions in some sites in the north. **e f g h** are the same as **a b c d** but for CO, while **i j k l** are for NO_2.

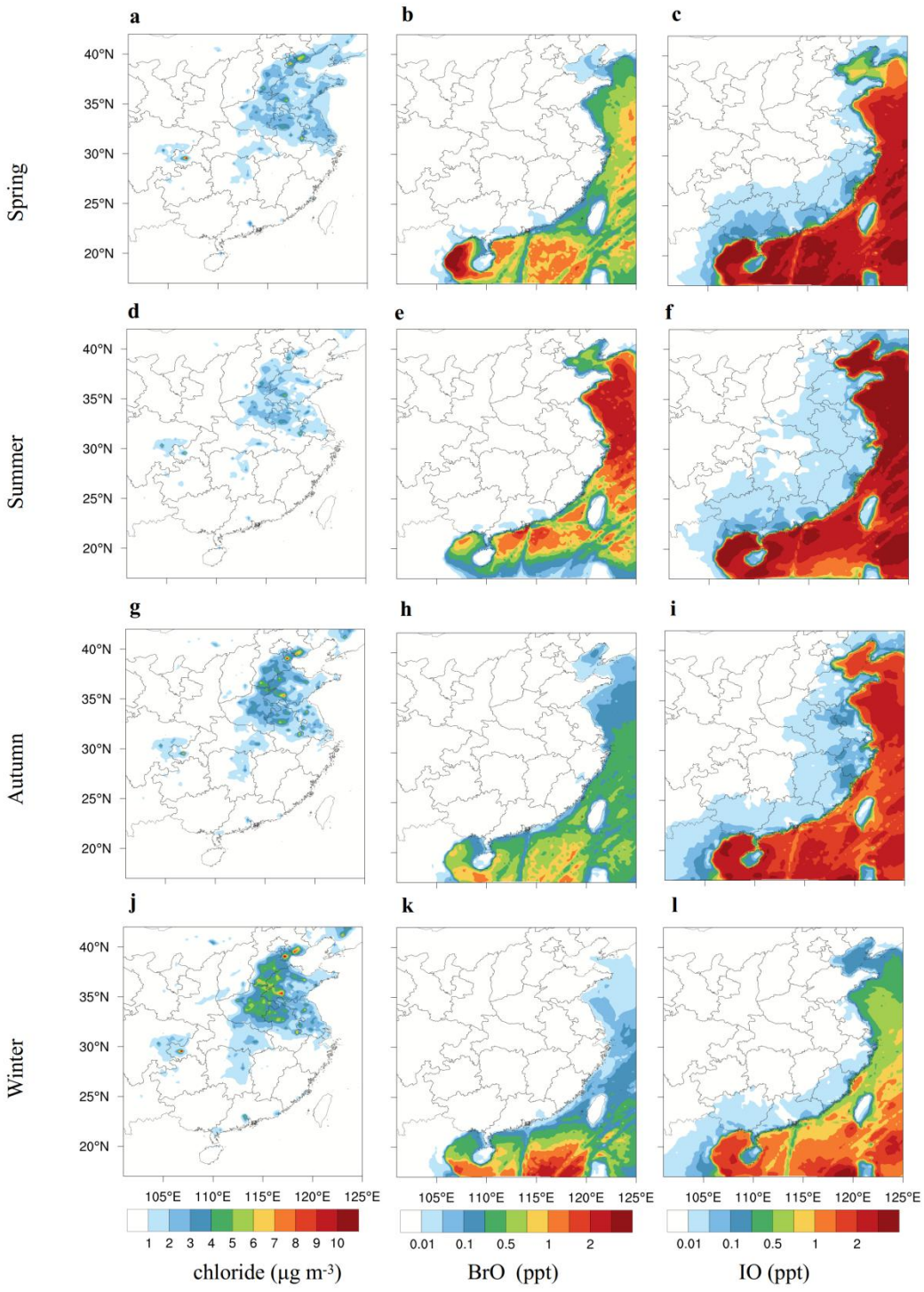

Figure S3 Seasonal average of daily-maximum of chloride aerosol (μg m^{-3}), BrO (ppt) and IO (ppt) simulated in the HAL scenario.

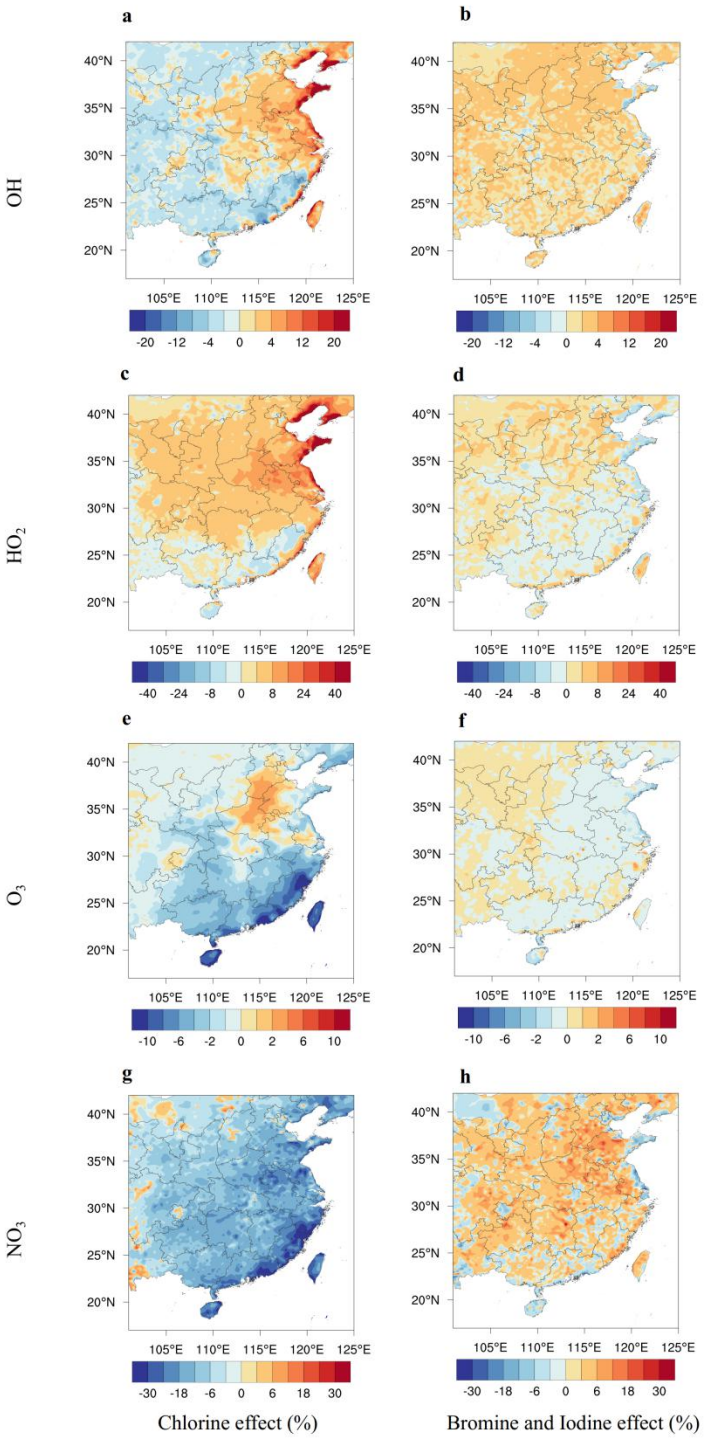

Figure S4 Seasonal average of relative changes of OH, HO_2, O_3, and NO_3 due to chlorine (difference between HAL-CHL), bromine and iodine (difference between CHL and HAL) in the four seasons

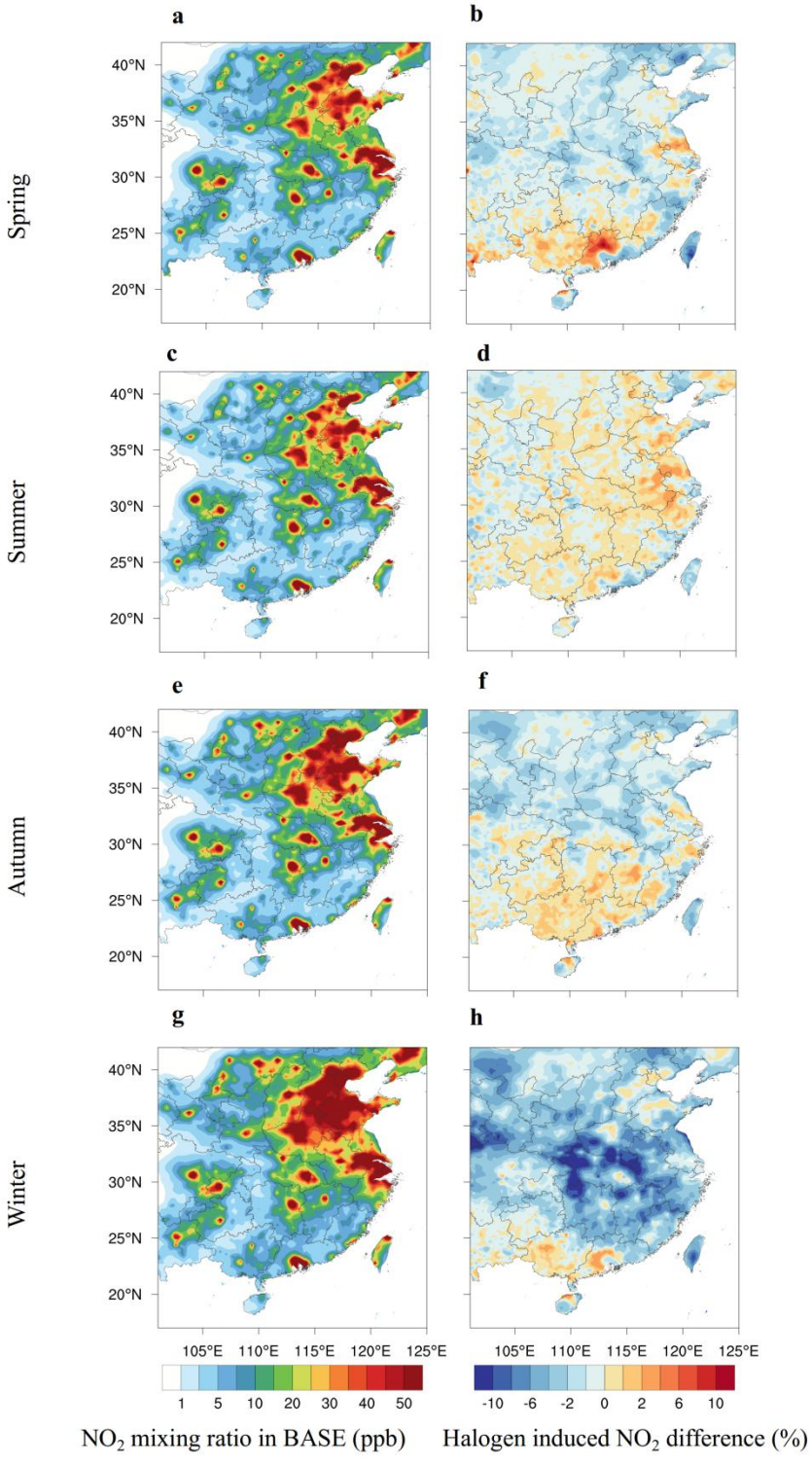

Figure S5 Seasonal average of daily-maximum NO_2 at the surface in the BASE scenario and relative changes due to halogens (difference between HAL-BASE) in the four seasons

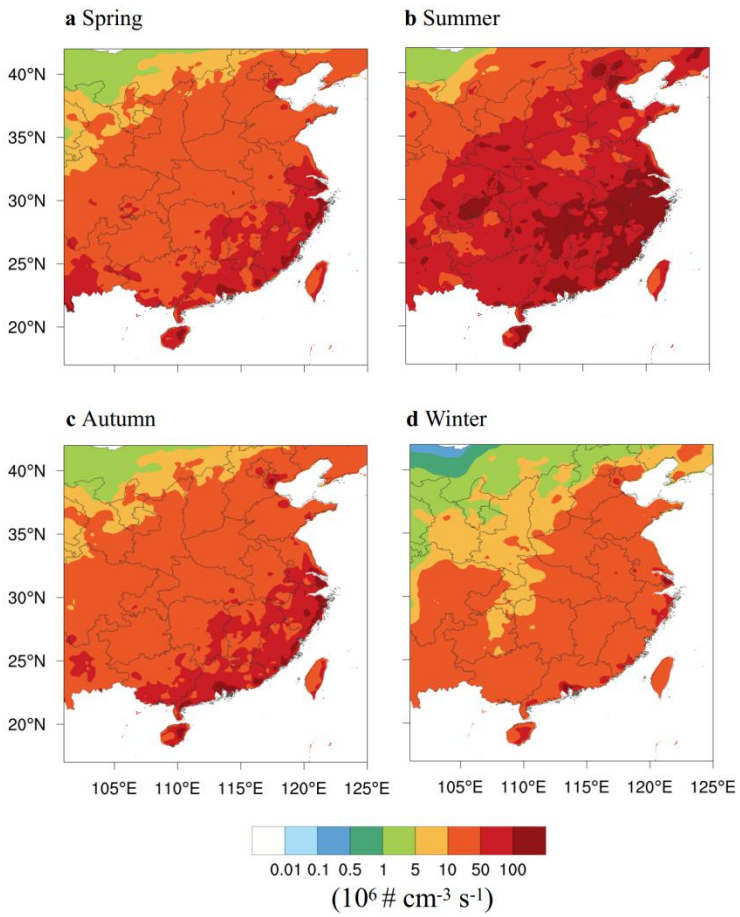

Figure S6 Seasonal average of AOC at the surface in the BASE case. AOC during summertime is the highest and that in winter is the lowest. AOC in southern China is more elevated than in the north.

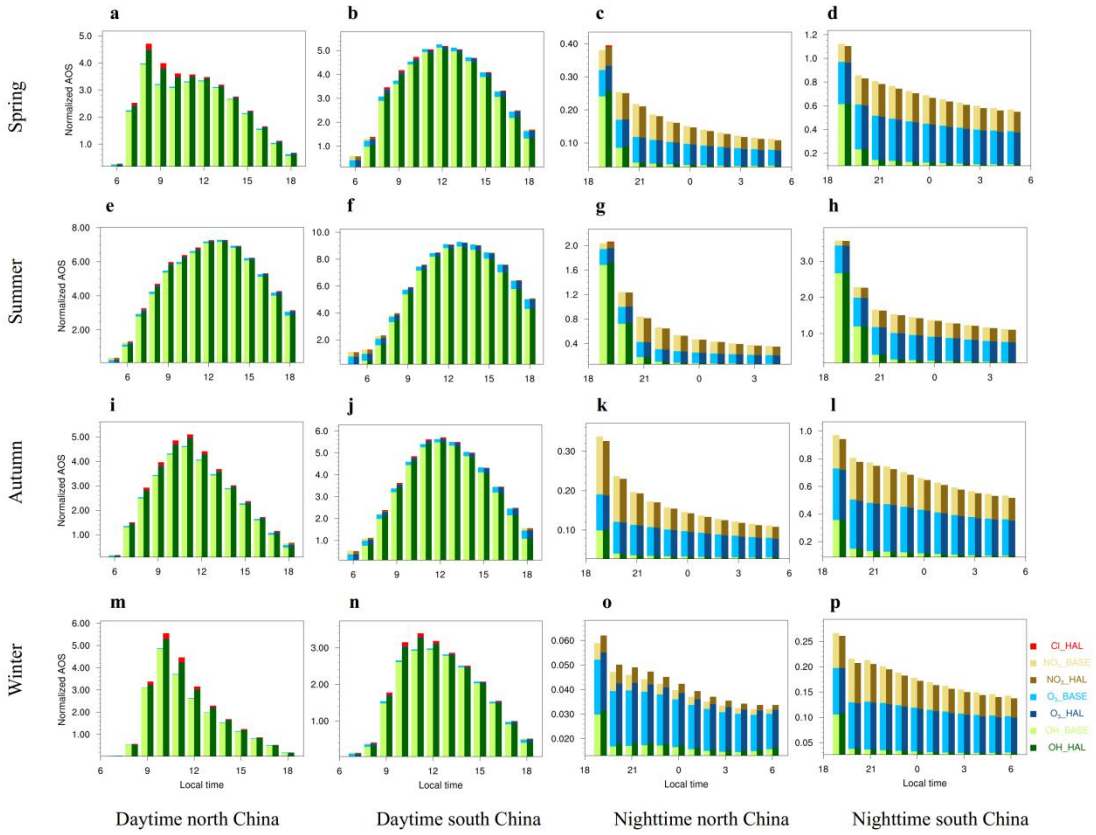

Figure S7 Daytime and nighttime hourly variations of AOC at the surface in north and south China in four seasons. The AOC is normalised by dividing the annual average AOC in China, 2.2×10^7 # cm^{-3} s^{-1}.

Table S1. Heterogeneous reactions of halogen species used in the WRF-Chem model

Heterogeneous reactions	Note	Uptake coefficient
ClNO3 →HOCl+HNO3	Hydrolysis	0.001[a]/0.01[b]
ClNO3 +HCl→Cl2 +HNO3		0.1
ClNO3 +HBr→BrCl+HNO3		0.1
HOBr+HCl→BrCl+H2O		0.1
HOBr+HBr→Br2 +H2O		0.1
HOBr→0.6Br2	Sea salt only if pH< 5.5	0.1
BrNO3 →HOBr+HNO3	Hydrolysis	0.03[a]/0.8[b]
BrNO3 →0.6Br2 +HNO3	Sea salt only if pH< 5.5	0.08
BrNO2 →0.6Br2 +HNO3	Sea salt only if pH< 5.5	0.04
INO3 →0.5IBr+0.5ICl+HNO3	Sea salt only if pH< 5.5	0.01
INO3 →0.5I2 +HNO3	Sea salt only if pH> 5.5	0.01
INO2 →0.5IBr+0.5ICl+HNO3	Sea salt only if pH< 5.5	0.02
INO2 →0.5I2 +HNO3	Sea salt only if pH> 5.5	0.02
HOI→0.5IBr+0.5ICl	Sea salt only if pH< 5.5	0.06
HOI→0.5I2	Sea salt only if pH> 5.5	0.06
I2O3 → I(aerosol)		0.02
I2O2 → I(aerosol)		0.02
I2O4 → I(aerosol)		0.02

[a] Uptake coefficient for moderate temperature.
[b] Uptake coefficient for cold temperatures.

Table S2 Reactions used to calculate the AOC

Reaction number	Reaction	Reaction rates
1	OH + CH3OOH	ARR2(3.8e-12, -200., TEMP) [a]
2	OH + CH2O	9.00E-12
3	OH + C2H4 + M	TROE(1.e-28 , .8 , 8.8e-12 , 0. , TEMP, C_M) [b]
4	OH + GLYOXAL	1.10E-11
5	OH + C2H6	ARR2(8.7e-12, 1070., TEMP)
6	OH + C2H5OOH	ARR2(3.8e-12, -200., TEMP)
7	OH + C3H6 + M	JPL_TROE(8.0e-27 , 3.5 , 3.e-11 , 0. , .5, TEMP, C_M) [c]
8	OH + POOH	ARR2(3.8e-12, -200., TEMP)
9	OH + CH3CHO	ARR2(5.6e-12, -270., TEMP)
10	OH + CH3COOOH	1.00E-12
11	OH + C3H8	ARR2(1.e-11, 660., TEMP)
12	OH + C3H7OOH	ARR2(3.8e-12, -200., TEMP)
13	OH + CH3COCH3	3.82e-11*exp(-2000./TEMP) + 1.33e-13
14	OH + BIGENE	5.40E-11
15	OH + BIGALK	3.50E-12
16	OH + ALKOOH	ARR2(3.8e-12, -200., TEMP)
17	OH + ONIT	6.80E-13
18	OH + MEK	ARR2(2.3e-12, 170., TEMP)
19	OH + MEKOOH	ARR2(3.8e-12, -200., TEMP)
20	OH + TOLOOH	ARR2(3.8e-12, -200., TEMP)
21	OH + ISOP	ARR2(2.54e-11, -410., TEMP)
22	OH + ISOPOOH	ARR2(1.52e-11, -200., TEMP)
23	OH + MVK	ARR2(4.13e-12, -452., TEMP)
24	OH + MACR	ARR2(1.86e-11, -175., TEMP)
25	OH + MACROOH	ARR2(2.3e-11, -200., TEMP)
26	OH + BENZENE	ARR2(2.3e-12, 193., TEMP)
27	OH + PHENOL	ARR2(4.7e-13, -1220., TEMP)
28	OH + PHENOOH	ARR2(3.8e-12, -200., TEMP)
29	OH + C6H5OOH	ARR2(3.8e-12, -200., TEMP)
30	OH + BENZOOH	ARR2(3.8e-12, -200., TEMP)
31	OH + TOLUENE	ARR2(1.7e-12, -352., TEMP)
32	OH + CRESOL	4.70E-11
33	OH + BZOOH	ARR2(3.8e-12, -200., TEMP)
34	OH + BZALD	ARR2(5.9e-12, -225., TEMP)
35	OH + XYLENES	1.70E-11
36	OH + XYLOL	8.40E-11
37	OH + XYLOLOOH	ARR2(3.8e-12, -200., TEMP)
38	OH + XYLENOOH	ARR2(3.8e-12, -200., TEMP)
39	OH + APIN	ARR2(1.2e-11, -440., TEMP)
40	OH + BPIN	ARR2(1.6e-11, -470., TEMP)

41	OH + LIMON	ARR2(4.2e-11, -400., TEMP)
42	OH + MYRC	2.10E-10
43	OH + BCARY	2.00E-10
44	OH + TERPOOH	3.30E-11
45	OH + CH3COOH	7.00E-13
46	OH + CH3COCHO	ARR2(8.4e-13, -830., TEMP)
47	OH + ONITR	4.50E-11
48	OH + HYDRALD	ARR2(1.86e-11, -175., TEMP)
49	OH + XOOH	ARR2(1.9e-12, -190., TEMP)
50	OH + CH3OH	ARR2(7.3e-12, 620., TEMP)
51	OH + C2H5OH	ARR2(6.9e-12, 230., TEMP)
52	OH + MPAN	JPL_TROE(8.e-27 , 3.5 , 3.e-11 , 0.0 , .5, TEMP, C_M)
53	OH + PAN	4.00E-14
54	OH + HYAC	3.00E-12
55	OH + GLYALD	1.00E-11
56	OH + MBO	ARR2(8.1e-12, -610., TEMP)
57	OH + HMPROP	1.40E-11
58	OH + MBOOOH	ARR2(3.8e-12 ,-200., TEMP)
59	OH + C2H2 + M	TROE(5.5e-30 , 0., 8.3e-13, -2., TEMP, C_M)
60	OH + HCOOH	4.50E-13
61	OH + CO	1.5e-13 * (1. + 6.e-7*1.38e-16*C_M*TEMP)
62	O3 + C2H4	ARR2(1.2e-14, 2630., TEMP)
63	O3 + C3H6	ARR2(6.5e-15, 1900., TEMP)
64	O3 + ISOP	ARR2(1.05e-14, 2000., TEMP)
65	O3 + MVK	ARR2(7.52e-16, 1521., TEMP)
66	O3 + MACR	ARR2(4.4e-15, 2500., TEMP)
67	O3 + APIN	ARR2(6.3e-16, 580., TEMP)
68	O3 + BPIN	ARR2(1.7e-15, 1300., TEMP)
69	O3 + LIMON	ARR2(3.0e-15, 780., TEMP)
70	O3 + MYRC	4.70E-16
71	O3 + BCARY	1.20E-14
72	O3 + MBO	1.00E-17
73	NO3 + CH2O	ARR2(6.e-13, 2058., TEMP)
74	NO3 + C3H6	ARR2(4.6e-13, 1156., TEMP)
75	NO3 + CH3CHO	ARR2(1.4e-12, 1900., TEMP)
76	NO3 + LIMON	1.10E-11
77	NO3 + MYRC	1.20E-11
78	NO3 + BCARY	1.90E-11
79	NO3 + ISOP	ARR2(3.03e-12, 446., TEMP)
80	NO3 + CH3COCHO	ARR2(1.4e-12, 1860., TEMP)
81	NO3 + ONITR	ARR2(1.4e-12, 1860., TEMP)
82	NO3 + MBO	ARR2(4.6e-14, 400., TEMP)

83	CL + CH2O	ARR3(8.1e-11,34.,TEMP) ;
84	CL + CH3CHO	8.00E-11
85	CL + CH3OH	5.50E-11
86	CL + CH3OOH	5.70E-11
87	CL + C3H8	ARR2(7.85e-11, 80.,TEMP) ;
88	CL + C2H6	ARR2(7.2e-11, 70.,TEMP) ;
89	CL + C3H6+O2	3.60E-12

Note:

[a] TEMP is the ambient air temperature.

ARR2(m,n,TEMP) = m * exp(-n/TEMP).

[b] C_M is the ambient air density in # cm $^{-3}$.

k0_t = k * (300/TEMP)^l * C_M.

kinf_t = m * (300/TEMP)^n.

kratio = k0_t/kinf_t.

TROE(k,l,m,n,TEMP,C_M) = k0_t/(1.0+kratio)*0.6^(1.0/(1.0+log10(k_ratio)^2)).

[c] k0_t = k * (300/TEMP)^l * C_M.

kinf_t = m * (300/TEMP)^n.

kratio = k0_t/kinf_t.

Table S3 Comparison of observed and simulated $ClNO_2$, BrO, Br_y, and IO in the HAL scenario

Species	Location (lat & lon)	Observation period	Observation average (pptv)	Simulation average [a] (pptv)	Reference
$ClNO_2$	Beijing (40.0, 116.4)	Jun, 2017	174.3	75 (75-283)	Zhou et al., 2018
	Heshan (22.7, 112.9)	Jan, 2017	1100.0	293 (36-293)	Yun et al., 2018
	Jinan (36.7, 117.0)	Aug-Sep, 2014	94.0	497 (208-906)	Wang X et al., 2017
	Mt. Tai (36.3, 117.1)	Jul-Aug, 2014	30.4	262 (202-895)	Wang Z et al., 2017
	Wangdu (38.7, 115.2)	Jun-Jul, 2014	159.5	272 (206-754)	Tham et al, 2016
	Mt. TMS (22.4, 114.1)	Nov-Dec, 2013	74.6 (nighttime)	146 (22-183) (nighttime)	Wang et al., 2016
	Hok Tsui (22.2, 114.3)	Aug, 2012	148.0	25 (14-131)	Tham et al., 2014
BrO	West Pacific	Jan-Feb, 2014	0.15 to 1.7 (daytime flight average< 500 m)	-	Koenig et al., 2017
Br_y	West Pacific	Jan-Feb, 2014	1.0 to 14.0 (daytime flight average< 500 m)	-	Koenig et al., 2017
IO	West Pacific	Oct, 2009	0.7 to 1.4 (daytime flight average in MBL)	-	Großmann et al., 2013;
	Global	2008-2013	0.4 to 1.4 (daytime average)	-	Prados-Roman et al., 2015

[a] The simulation results for $ClNO_2$ are the averages in the corresponding months with the range of monthly averages in parentheses. Direct observations of BrO and IO are not available in our domain, and we thus compared our simulated results with observations made in similar environments, i.e. the western Pacific. Daytime averages of BrO in months of Jan and Feb at lower boundary layer in west Pacific were typically in the range of 0.01 to 1.5 pptv, and those of Bry were between 0.5 and 8 pptv. Daytime averages of IO in the month of October in marine boundary layer were typically between 0.75 to 2.5 pptv. The simulations are generally in line with observations in similar environments.